Hereditary spastic paraplegia proteins REEP1, spastin, and atlastin-1 coordinate microtubule interactions with the tubular ER network

Seong H. Park,[1] Peng-Peng Zhu,[1] Rell L. Parker,[1,2] and Craig Blackstone[1]

[1]Cellular Neurology Unit, Neurogenetics Branch, National Institute of Neurological Disorders and Stroke (NINDS), NIH, Bethesda, Maryland.
[2]Howard Hughes Medical Institute–NIH Research Scholars Program, Bethesda, Maryland.

Hereditary spastic paraplegias (HSPs; SPG1–45) are inherited neurological disorders characterized by lower extremity spastic weakness. More than half of HSP cases result from autosomal dominant mutations in atlastin-1 (also known as *SPG3A*), receptor expression enhancing protein 1 (REEP1; *SPG31*), or spastin (*SPG4*). The atlastin-1 GTPase interacts with spastin, a microtubule-severing ATPase, as well as with the DP1/Yop1p and reticulon families of ER-shaping proteins, and SPG3A caused by atlastin-1 mutations has been linked pathogenically to abnormal ER morphology. Here we investigated SPG31 by analyzing the distribution, interactions, and functions of REEP1. We determined that REEP1 is structurally related to the DP1/Yop1p family of ER-shaping proteins and localizes to the ER in cultured rat cerebral cortical neurons, where it colocalizes with spastin and atlastin-1. Upon overexpression in COS7 cells, REEP1 formed protein complexes with atlastin-1 and spastin within the tubular ER, and these interactions required hydrophobic hairpin domains in each of these proteins. REEP proteins were required for ER network formation in vitro, and REEP1 also bound microtubules and promoted ER alignment along the microtubule cytoskeleton in COS7 cells. A *SPG31* mutant REEP1 lacking the C-terminal cytoplasmic region did not interact with microtubules and disrupted the ER network. These data indicate that the HSP proteins atlastin-1, spastin, and REEP1 interact within the tubular ER membrane in corticospinal neurons to coordinate ER shaping and microtubule dynamics. Thus, defects in tubular ER shaping and network interactions with the microtubule cytoskeleton seem to be the predominant pathogenic mechanism of HSP.

Introduction

Hereditary spastic paraplegias (HSPs) comprise a group of inherited neurological disorders with the cardinal feature of progressive spasticity and weakness of the lower extremities, due to a length-dependent axonopathy of corticospinal motor neurons (1–5). HSPs have historically been classified as pure if spastic paraparesis occurs in isolation and complicated if other neurological abnormalities are present (6). More recently, a molecular genetic classification has come into wide use, with over 40 different genetic loci (*SPG1–45*) reported (7). The identification of genes for 20 of these HSPs has stimulated development of a classification scheme based on possible pathogenic mechanisms. These include mitochondrial dysfunction, abnormalities in axonal pathfinding or myelination, and intracellular trafficking defects (1–5). A majority of HSP gene products have been implicated generally in intracellular membrane and protein trafficking (3), though in most cases conclusive mechanistic insights are lacking.

Despite the daunting number of distinct genetic loci, well over 50% of HSP patients harbor pathogenic mutations in 1 of just 3 genes: spastin (*SPG4*, also known as *SPAST*), atlastin-1 (*SPG3A*, also known as *ATL1*), or receptor expression enhancing protein 1 (REEP1, also known as *SPG31*). Recently, we demonstrated that the atlastin-1 protein is a member of a class of dynamin-related GTPases present in all eukaryotes that includes 3 highly related proteins in humans (atlastin-1, atlastin-2, and atlastin-3) as well as *Saccharomyces cerevisiae* synthetic enhancer of *yop1* (Sey1p) and *Arabidopsis* root hair defective 3 (RHD3) (8). This ubiquitous protein family functions in the generation of the tubular ER network in eukaryotes, with a critical role in the formation of 3-way junctions (8, 9), by mediating homotypic fusion of ER tubules (10).

The ER is a continuous membrane system that comprises the inner and outer nuclear membranes as well as peripheral ER sheets and a network of interconnected tubules (11, 12). The atlastin-1 GTPase localizes prominently to the tubular ER, in which it interacts with 2 families of ER-shaping proteins, the reticulons and DP1/Yop1p (DP1 is also known as REEP5) (8). These ER-shaping proteins likely deform the lipid bilayer into high-curvature tubules through hydrophobic insertion (wedging) and scaffolding mechanisms by occupying more space in the outer than the inner leaflet of the ER lipid bilayer via their membrane-inserted, double-hairpin hydrophobic domains (8, 13–16). Both GTP-binding and *SPG3A* missense mutations in atlastin-1 act in a dominant-negative manner to disrupt formation of the tubular ER network in cells and impair axon elongation in neurons (8, 9, 17).

Atlastin-1 interacts with the *SPG4* protein spastin, an ATPase associated with diverse cellular activities (AAA) that functions in microtubule severing and exerts prominent effects on axon branching and elongation in neurons (18–21). Spastin exists in 2 isoforms generated through the use of different translation ini-

Conflict of interest: The authors have declared that no conflict of interest exists.
Citation for this article: *J Clin Invest.* 2010;120(4):1097–1110. doi:10.1172/JCI40979.

tiation sites, commencing at residues 1 (M1 isoform; 68 kDa) or 87 (M87 isoform; 60 kDa) (22). Atlastin-1 interacts only with the larger M1 spastin that harbors a hydrophobic domain and localizes to the ER (23–25). M1 spastin is enriched in brain and particularly in spinal cord (20, 22), and expression of an ATPase-defective form of M1 spastin that also represents a known pathogenic *SPG4* mutation, p.K388R (26), results in thickened, bundled microtubules that associate with and redistribute the ER tubules (25). In addition, the *SPG31* protein REEP1 is structurally similar to the DP1/Yop1p proteins that shape ER tubules and bind atlastin-1, suggesting a broader role for ER-shaping defects in the pathogenesis of the HSPs (8, 27, 28). However, though a number of studies have suggested that REEP1 localizes to the ER (29, 30), a recent report has proposed that it is mitochondrial (31).

In this study, we have investigated the distribution, protein interactions, and function of the REEP1 protein. We demonstrate that REEP1 localizes prominently to the tubular ER, in which it interacts with both atlastin-1 and spastin through an intramembrane, hydrophobic hairpin domain. Unexpectedly, REEP1 also mediates interaction of the tubular ER with microtubules, which to our knowledge identifies REEP1 as a member of a novel protein family within the DP1/Yop1p superfamily. A truncated REEP1 protein resulting from a pathogenic *SPG31* mutation does not bind microtubules, and it disrupts the ER network. We present a model proposing that these 3 common HSP proteins — atlastin-1, spastin, and REEP1 — interact with one another to coordinate shaping of the ER tubules and ER-microtubule interactions to construct the tubular ER network. We suggest ER network defects as the predominant pathogenic mechanism for the HSPs.

Results

REEP1 is an ER protein within the DP1/Yop1p superfamily. We undertook a systematic analysis of the structure, biochemical properties, and distribution of REEP1, beginning with its phylogenetic relationships. Most species have a number of closely related REEP/DP1/Yop1p superfamily members; for instance, there are 6 in humans and other mammals (REEP1–6) (Figure 1A). The budding yeast *S. cerevisiae* has only 1 member, Yop1p; however, for other species, there is a clear phylogenetic delineation of REEP proteins into 2 distinct subfamilies based on sequence similarity, comprising REEP1–4 and REEP5–6 in higher species (Figure 1A). In fact, though all REEPs harbor paired hydrophobic domains, REEP1–4 are characterized by the presence of a much shorter first hydrophobic segment, lack of a clear N-terminal cytoplasmic domain, and a longer C-terminal region relative to REEP5–6 (Figure 1A and Supplemental Figures 1 and 2; supplemental material available online with this article; doi:10.1172/JCI40979DS1). Importantly, even species such as the fruit fly *Drosophila*, sea urchin *Strongylocentrotus purpuratus*, and worm *Caenorhabditis elegans* have at least one REEP protein each with similarity to REEP1–4 and REEP5–6. Yeast Yop1p is structurally most similar to REEP5–6, presenting the possibility that REEP1–4 proteins have functions distinct from, or in addition to, the fundamental ER-shaping roles described for mammalian REEP5–6 and yeast Yop1p (13).

We generated antipeptide antibodies against human REEP1 for biochemical and immunocytochemical studies, with the antigenic peptide sequence selected to avoid cross-reactivity with other human REEP family members (Supplemental Figure 1). Though endogenous REEP1 protein and mRNA were not detectable by immunoblotting or RT-PCR, respectively, in HEK293 cells or COS7 cells (Figure 1B and Supplemental Figure 3), consistent with a previous report (30), REEP1 was readily observed upon overexpression in these cells (Figure 1B). The robust REEP1-immunoreactive signal at approximately 22 kDa on immunoblots was substantially diminished by REEP1 siRNA treatment (Figure 1C). An endogenous protein band of the same size was identified in rat brain and spinal cord homogenates, with an additional higher MW protein, of approximately 29 kDa (Figure 1B), that could represent either a cross-reacting band or a modified form of REEP1. Similar patterns of immunoreactivity were present on immunoblots of 2-dimensional protein gels, resolving extracts from HeLa cells overexpressing REEP1, and extracts from adult rat cerebral cortical tissue, and the presence of multiple corresponding protein spots reinforces the likelihood of posttranslational modifications in REEP1 (Supplemental Figure 4).

Members of the DP1/Yop1p protein family form higher-order oligomeric structures (15). REEP1 forms higher-order oligomers as well, as shown on immunoblots of nonreducing SDS-PAGE gels after chemical cross-linking with dithiobis(succinimidyl propionate) (DSP), and these cross-linked products can be efficiently cleaved with the reducing agent DTT (Figure 1D). REEP1 harbors 2 hydrophobic regions, which, by their relationship with DP1/Yop1p and reticulon proteins (13), may sit as paired hairpins inserted into the membrane lipid bilayer. Consistent with this prediction, REEP1 associates with membranes during subcellular fractionation (Figure 1E), and we established that REEP1 is an integral membrane protein, using both alkaline membrane extraction and Triton X-114 detergent phase partitioning (Figure 1, F and G).

We considered the possibility that the N-terminal 20 aa of REEP1 might represent a signal peptide that could be cleaved by signal peptidase and thus not be present in the mature protein. An expression construct for a REEP1 protein lacking aa 1–20, with an initiator Met at residue 21 (ΔN-REEP1), was generated to mimic the size of a putative processed protein. However, on SDS-PAGE gels, ΔN-REEP1 clearly migrated at a MW several kDa smaller than WT REEP1, indicating that the N-terminal hydrophobic domain was not a cleaved signal peptide and thus is present in the mature protein (Figure 1H). Protease protection studies employing proteinase K treatment of intact microsomes from HEK293 cells overexpressing REEP1 demonstrated that the REEP1 C terminus faces the cytoplasm, while the ER luminal protein Grp78 remained undigested by protease and only the cytoplasmic portion of the membrane-spanning protein calnexin was cleaved, as expected (Figure 1I). Taken together, these data are consistent with either of the 2 REEP1 membrane topology models shown in Figure 1J. The model on the left is based on that proposed for other ER-shaping proteins in the DP1/Yop1p protein superfamily, in particular REEP5–6 and Yop1p (Figure 1K and ref. 13). Since the first hydrophobic segment of REEP1–4 is not as large as that in REEP5–6 (Supplemental Figures 1 and 2), we have also presented the possibility that the first hydrophobic segment in REEP1–4 is a more traditional membrane-spanning segment (Figure 1J), though the presence of conserved Arg/Lys (in REEP1–4) and Pro residues (REEP1–6) within this otherwise hydrophobic domain would be unusual for a typical transmembrane segment (Supplemental Figures 1 and 2).

REEP1–4 proteins are required for ER network formation. Previous studies have established a direct role for mammalian REEP5/DP1 and yeast Yop1p in shaping ER tubules (13). Since REEP1–4 proteins exhibit structural differences when compared with the REEP5–6 proteins, as described above, we examined the role of

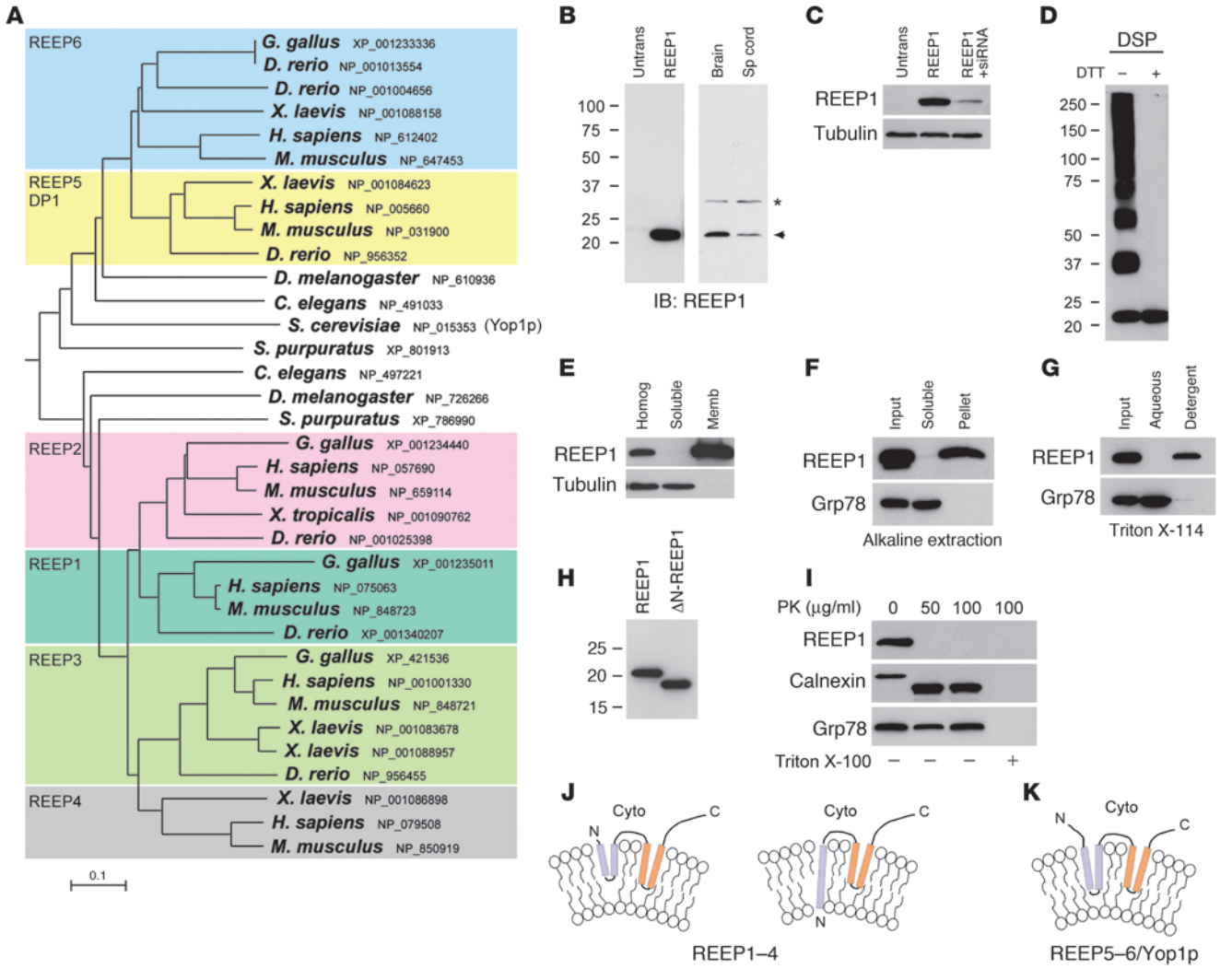

Figure 1

REEP1 is in the DP1/Yop1p superfamily of ER-shaping proteins. (**A**) REEP/DP1/Yop1p protein phylogeny. A ClustalW (version 1.4) tree with species name and GenBank protein accession numbers are shown. REEP1–6 are color coded. The scale bar denotes the number of substitutions per site. (**B**) Expression of REEP1. Untransfected HEK293 cells (Untrans), cells overexpressing REEP1, and rat brain and spinal cord (Sp cord) homogenates were immunoblotted for REEP1. An arrowhead indicates REEP1; an asterisk identifies modified REEP1 or a cross-reacting protein. MW standards (in kDa) are indicated throughout. (**C**) REEP1 antibody specificity. Cells overexpressing REEP1 were transfected with control or REEP1-specific siRNA and immunoblotted for REEP1. β-Tubulin was monitored as a loading control. (**D**) Oligomerization of REEP1. Extracts from REEP1-expressing cells were cross-linked with DSP and resolved by SDS-PAGE on nonreducing gels with or without DTT, which cleaves cross-links. (**E**) REEP1 membrane association. Homogenates (Homog) from REEP1-expressing cells were separated into soluble and membrane (Memb) fractions then immunoblotted for REEP1 or the cytoplasmic protein β-tubulin. (**F**) Alkaline membrane extraction. Lysed membranes from REEP1-expressing cells (Input) were alkaline extracted, and soluble and pellet fractions were immunoblotted for REEP1 and the soluble protein Grp78. (**G**) Detergent phase partitioning. Membranes from REEP1-expressing cells were partitioned with Triton X-114. Input membranes as well as detergent and aqueous phases were immunoblotted. (**H**) Cells overexpressing REEP1 and ΔN-REEP1 (lacking aa 1–20) were immunoblotted for REEP1. (**I**) Protease protection. Proteinase K (PK) was added to intact microsomes from REEP1-expressing cells with or without Triton X-100, and aliquots were immunoblotted. (**J**) Two possible topology models for REEP1–4. (**K**) Topology model for REEP5–6/Yop1p. Cyto, cytoplasm.

REEP1–4 proteins in shaping the ER. We employed an in vitro assay for ER network formation that uses a microsomal vesicle fraction isolated from *Xenopus* eggs (8, 13, 32). Upon the addition of GTP, these vesicles formed intricate networks in vitro (Figure 2, A and B). Preincubation of the membranes with control rabbit IgG prior to addition of GTP did not affect this network generation (Figure 2C), though equimolar concentrations of rabbit polyclonal antibodies against the atlastin GTPases in *Xenopus* abolished the tubular network formation (Figure 2D), as reported previously (8). Using antibodies directed against 2 different regions within *Xenopus* REEP1–4 proteins (Supplemental Figure 2), we visualized dramatic inhibition of ER network formation (Figure 2, E and F). In additional control experiments, antibodies directed against the ER membrane proteins inositol triphosphate receptor (IP_3R) and TRAPα did not affect

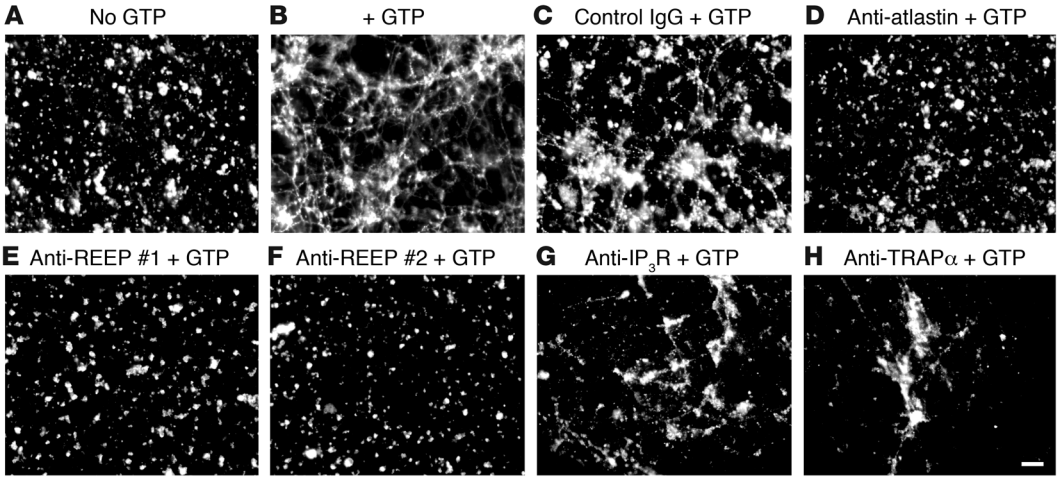

Figure 2
Anti–REEP1–4 antibodies inhibit ER network formation in vitro. (**A** and **B**) Membranes from *Xenopus* eggs were incubated in the absence (**A**) or presence (**B**) of GTP for 1 hour, stained with octadecyl rhodamine, and visualized by confocal fluorescence microscopy. (**C**–**H**) As in **B**, except membranes were preincubated for 1 hour with 1.1 μM control IgG (**C**), affinity-purified pan-atlastin antibodies (**D**), either of 2 different affinity-purified anti-REEP antibodies (**E** and **F**), anti-IP_3R antibodies (**G**), or anti-TRAPα antibody (**H**) prior to addition of GTP. Scale bar: 20 μm.

the in vitro network formation (Figure 2, G and H), as reported previously (13). These data establish that the REEP1–4 proteins, like REEP5–6, are directly involved in ER shaping.

REEP1 links ER tubules to the microtubule cytoskeleton. To determine the subcellular distribution of REEP1, we compared its localization to markers for the ER, *cis/medial*-Golgi apparatus, and mitochondria in COS7 cells, with visualization using confocal immunofluorescence microscopy. REEP1 did not colocalize with the mitochondrial marker Mito-DsRed, but colocalized extensively with the ER protein Sec61β (Figure 3A), consistent with the in vitro data in Figure 2. The Golgi apparatus, as assessed by staining for endogenous GM130, appeared fragmented upon REEP1 overexpression, but colocalization of GM130 with REEP1 was very limited (Figure 3A). Interestingly, REEP1 overexpression caused dramatic alterations in ER morphology, with a distribution pattern similar to that of ER tubules aligned along thickened and bundled microtubules. This pattern was consistently visualized over a broad range of REEP1 expression levels (Figure 3A and data not shown). To establish whether this phenotype required coexpression of both REEP1 and Sec61β, we examined the effects of REEP1 expression alone on the distribution of the endogenous ER protein calnexin in another cell type, HeLa cells (Figure 3B). The results obtained were similar to those shown in Figure 3A. Thus, REEP1 overexpression alone was sufficient to induce this ER phenotype (Figure 3B) in the absence of any changes in overall cellular levels of β-tubulin or calnexin (Figure 3C). In cells overexpressing REEP1, the ER closely aligned with the microtubule cytoskeleton, as revealed by staining for β-tubulin (Figure 3E). Consistent with these localization studies, in vitro microtubule-binding assays using extracts from cells overexpressing REEP1 revealed that REEP1 coprecipitates with polymerized microtubules (Figure 3D).

To determine whether the bundling of microtubules along the rearranged tubular ER was a property shared by all the REEP1–4 proteins, we overexpressed the closely related REEP2 protein, which is present in these cell types endogenously (ref. 30 and data not shown), and compared the ER morphology with that in cells overexpressing REEP5 or REEP6, with each of the proteins similarly tagged with the HA epitope at the C terminus. While REEP1 and REEP2 exhibited very similar patterns of ER redistribution along thickened and bundled microtubules, both REEP5 and REEP6 expression resulted in a more typical ER network and a largely unaffected microtubule cytoskeleton, with microtubules radiating from the microtubule-organizing center (Supplemental Figure 5).

SPG31 mutant REEP1 does not bind microtubules and disrupts the ER network. A number of *REEP1* mutations are nonsense mutations, resulting in premature protein truncation (33–35). We investigated one nonsense *SPG31* mutation in exon 5, c.337C>T (p.Arg113X), that results in premature truncation of REEP1 after residue 112, but which fully retains the 2 hydrophobic domains (ref. 35 and Supplemental Figure 1). This truncated REEP1 still forms higher-order oligomers, as assessed using chemical cross-linking with DSP (Supplemental Figure 6A). However, upon expression in COS7 cells, the SPG31 mutant REEP1 showed clear differences in subcellular localization compared with WT REEP1, demonstrating no colocalization with β-tubulin but retaining a highly overlapping distribution with Sec61β (Figure 4, A, B, and E). This finding was consistent with results of microtubule-binding assays, which clearly revealed that SPG31-truncated REEP1 in cell lysates is unable to associate with polymerized microtubules, in marked contrast with WT REEP1 (Figure 4C). Together, these data show that the cytoplasmic C terminus of REEP1 is required for microtubule interactions, though not necessarily that the interaction is direct. Upon overexpression of Sec61β, a typical interconnected ER network is visualized within COS7 cells (Figure 4D). Interestingly, this network is still partially formed, but clearly very disrupted, in cells coexpressing SPG31 mutant REEP1 with Sec61β. Despite the fact that these proteins colocalize closely, the ER network is not formed properly, with a large number of apparent vesicles and peripheral ER sheets and far fewer identifiable tubular interconnections (Figure 4, E and F).

To establish whether the REEP1 C terminus is sufficient for direct interaction with microtubules, we performed an in vitro cosedimen-

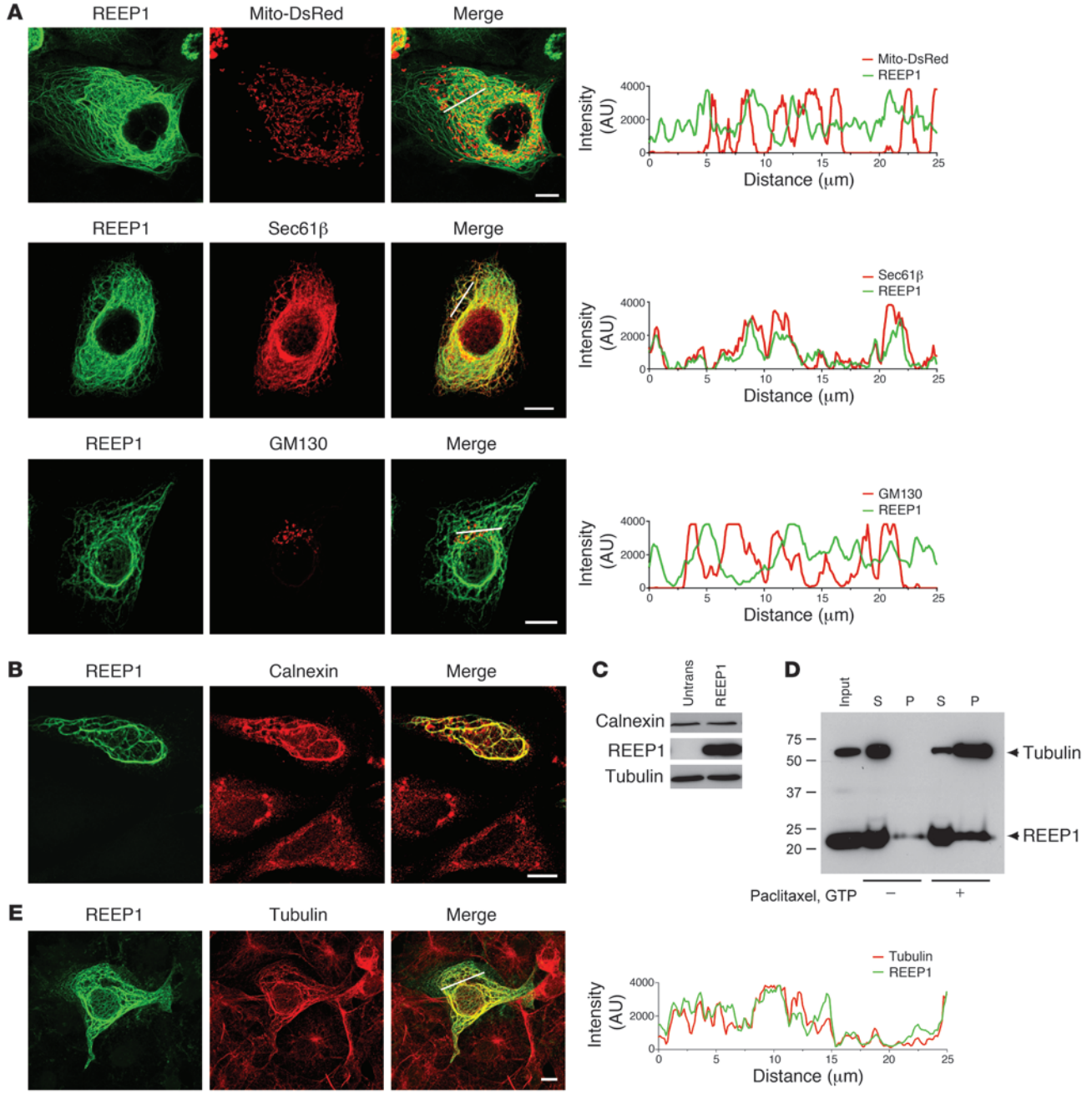

Figure 3

REEP1 expression increases ER alignment along microtubules. (**A**) REEP1 is an ER protein. COS7 cells coexpressing REEP1 (green) and Mito-DsRed (red; top row), the ER protein RFP-Sec61β (red; middle row), or REEP1-expressing cells costained for the *cis*/*medial*-Golgi maker GM130 (red; bottom row) were imaged using confocal microscopy. Relative fluorescence intensities for the indicated linear regions in merged images were measured using Zeiss LSM510 software and are graphed. Note the high degree of REEP1 and Sec61β line scan overlap but lack of significant overlap between REEP1 and Mito-DsRed or GM130. (**B**) HeLa cells were transfected with REEP1 and costained for REEP1 (green) and endogenous calnexin (red). Two untransfected cells are present at the bottom of the image for comparison. (**C**) Aliquots of untransfected and REEP1-transfected cells were immunoblotted for calnexin, REEP1, and β-tubulin. (**D**) REEP1 interaction with microtubules. REEP1 levels are markedly increased in the pellet (P), along with tubulin, upon addition of paclitaxel and GTP to cell lysates. S, soluble fraction. (**E**) COS7 cells were transfected with REEP1 and costained for REEP1 (green) and endogenous β-tubulin (red). Note the high degree of line scan overlap. Scale bars: 10 μm.

tation assay, using affinity-purified, GST-tagged REEP1 (aa 113–201) with purified microtubules. We found that although untagged GST did not coprecipitate with polymerized microtubules, a substantial portion of GST-REEP1 (aa 113–201) coprecipitated with polymerized microtubules, demonstrating a direct interaction (Figure 5). Taken together, these data indicate that REEP1 is an ER-shaping protein that also remodels the ER network by interacting through its C-terminal cytoplasmic domain directly with microtubules.

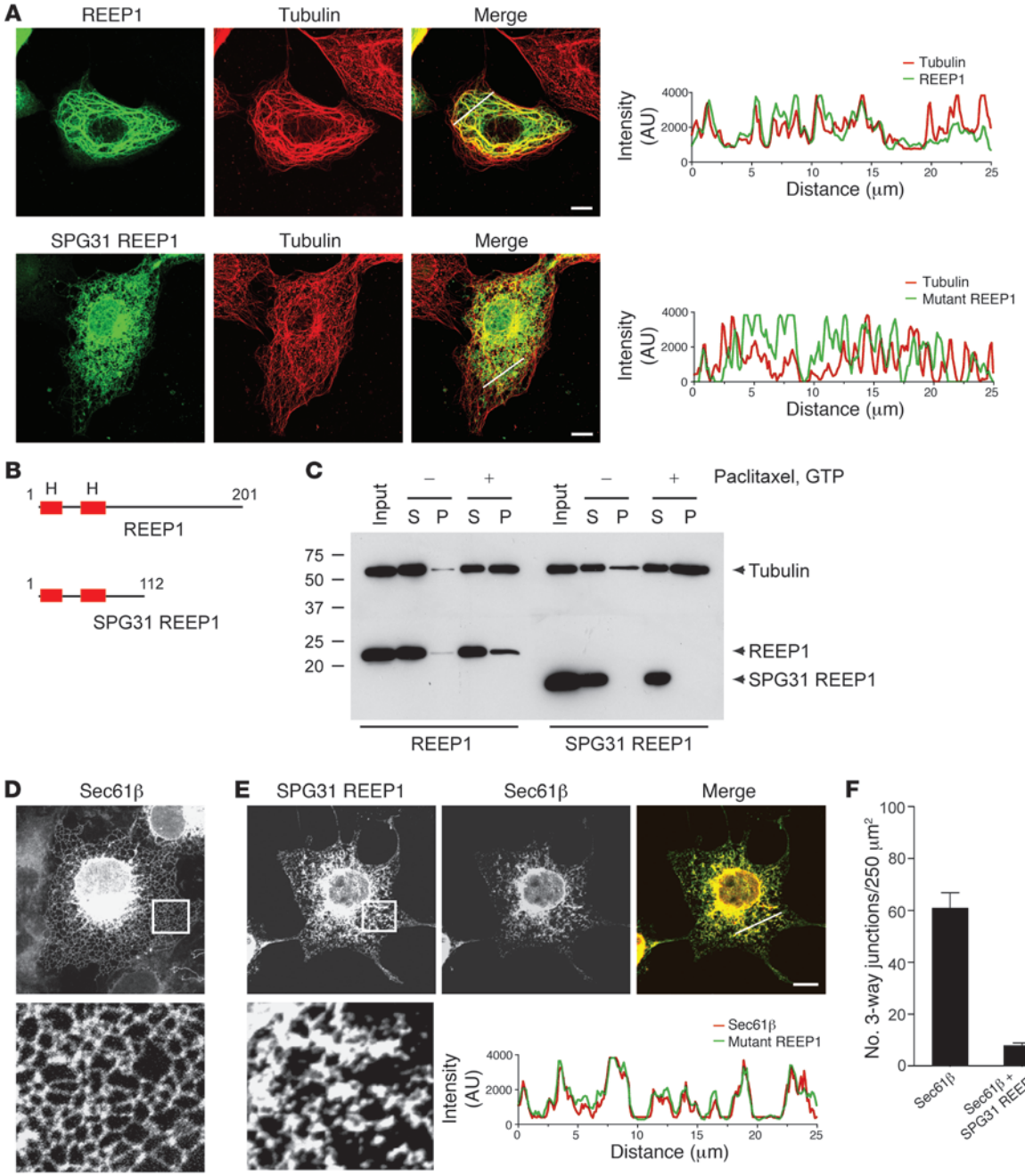

Figure 4

SPG31 REEP1 truncation mutant does not interact with microtubules and impairs ER reticularization. (**A** and **B**) SPG31 mutant REEP1 (aa 1–112) does not colocalize with the microtubule cytoskeleton. (**A**) COS7 cells were transfected with WT (top row) or mutant (bottom row) REEP1 and costained for β-tubulin (red), with merged images and line scan plots shown. (**B**) A schematic diagram of the REEP1 forms. (**C**) Mutant REEP1 does not interact with microtubules. Microtubule-binding assays show clear enrichment of WT REEP1 in the pellet fraction of extracts from cells preincubated with paclitaxel and GTP. Mutant REEP1 remains in the soluble fraction even after addition of paclitaxel and GTP. MW standards (in kDa) are indicated. (**D**) Cells overexpressing GFP-Sec61β exhibit a typical ER network, as revealed with confocal fluorescence microscopy. (**E**) Cells coexpressing Sec61β and mutant REEP1 exhibit a disrupted ER, with loss of both 3-way junctions and tubular appearance, despite the extensive colocalization of REEP1 (green) and RFP-Sec61β (red), as shown in the merged image and line scan plot. (**D** and **E**) Boxed areas are enlarged in the panels below (original magnification, ×5.7). (**F**) SPG31 mutant REEP1 expression inhibits formation of 3-way ER junctions. Number of 3-way junctions in cells in similar 250 μm² areas from **D** and **E** were counted (mean ± SD of 4 regions per trial, $n = 3$ trials for each condition; $P < 0.001$). Scale bars: 10 μm.

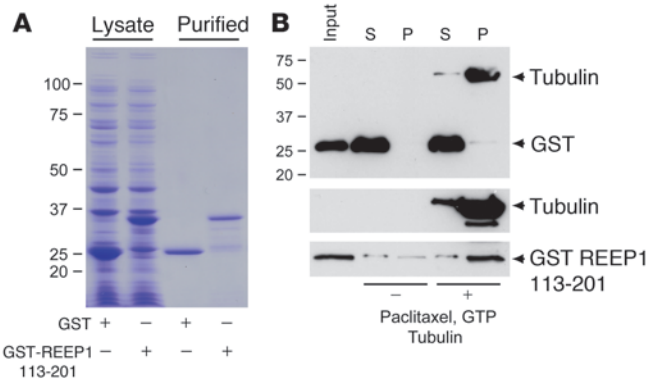

Figure 5

REEP1 C-terminal cytoplasmic domain is sufficient for microtubule interaction in vitro. (**A**) GST fusion protein production. Aliquots of crude bacterial lysates and affinity-purified GST and GST-REEP1 (aa 113–201) fusion proteins are shown, with detection by Coomassie Brilliant Blue staining after SDS-PAGE. MW standards (in kDa) are indicated. (**B**) REEP1 interaction with polymerized microtubules. GST-REEP1 (aa 113–201) levels are markedly increased in the pellet, along with tubulin, upon addition of paclitaxel and GTP to purified microtubules, while GST remains in the soluble fraction. The lower 2 panels represent immunoblots from the same gel, with detection of GST-REEP1 (aa 113–201) using anti-REEP1 antibodies.

REEP1 interacts with the HSP proteins atlastin-1 and spastin through intramembrane hairpin domains. Since the studies discussed thus far investigated REEP1 distribution in cells using overexpressed proteins, we established the endogenous localization of REEP1 in rat cerebral cortical neurons in primary culture, a preparation enriched in pyramidal neurons of the type affected in the HSPs. The anti-REEP1 antibody detected a single endogenous, approximately 22-kDa protein band of the appropriate size in extracts from cultured cerebral cortical neurons (Figure 6A). Immunocytochemical studies revealed endogenous REEP1 within ER in the cell soma and enriched within axonal varicosities and growth cones (Figure 6B and Supplemental Figure 7A). There was extensive REEP1 immunoreactivity in the cell body that appeared to colocalize with p115, a marker for ER-Golgi intermediate complexes (ERGICs) and *cis*-Golgi apparatus (Supplemental Figure 7B), though Grp78 staining was also enriched in this perinuclear area (Supplemental Figure 7A). The overall distribution of endogenous REEP1 was reminiscent of that reported in our previous studies of atlastin-1 in cultured cortical neurons (17), and indeed REEP1 and atlastin-1 colocalized very closely in these neurons, including within axonal varicosities and growth cones (Figure 6B). Similarly, spastin and REEP1 colocalized extensively in the neuronal soma as well as in axonal varicosities and growth cones (Figure 6C). However, REEP1 did not colocalize with the mitochondrial protein cytochrome *c* (Supplemental Figure 7C).

When the REEP1 and atlastin-1 proteins were overexpressed individually in COS7 cells, the resulting ER morphology, as assessed by coexpression with Sec61β, appeared different. REEP1-overexpressing cells showed fairly homogeneous REEP1 distribution along ER membrane tubules aligned with bundled, thickened microtubules. On the other hand, atlastin-1–expressing cells exhibited a more highly branched ER, with punctuate enrichment of atlastin-1 along the tubules, particularly at branch points in the cell periphery and within some aberrant ER sheets more centrally (Figure 7A) (8). Upon coexpression of atlastin-1 with REEP1, distinct atlastin-1 puncta were distributed along the more tubular staining pattern of REEP1, with the altered ER distributed along bundled microtubules (Figure 7B). The colocalization of REEP1 and atlastin-1 in puncta distributed along the ER tubules suggested that these proteins might interact directly, and, in fact, coimmunoprecipitation studies demonstrated that Myc-tagged atlastin-1 binds to REEP1 (Figure 7C).

The atlastins (comprising atlastin-1, atlastin-2, and atlastin-3 in humans) interact with tubule-shaping DP1/Yop1p and reticulon proteins through their respective intramembrane hydrophobic domains (8). Similarly, atlastin-1 interaction with REEP1 occurs through a C-terminal fragment of atlastin-1, harboring the paired membrane-spanning segments (aa 449–558; atlastin-1 TM) but not the large N-terminal cytoplasmic region that harbors the GTP-binding domain (aa 1–447; atlastin-1 Ncyt) (Figure 7D), a result consistent with colocalization studies in cells expressing these same fragments (Figure 7E). Furthermore, the SPG31 mutant REEP1 truncated after residue 112, but which harbors both hydrophobic domains, still interacted with the atlastin-1 TM fragment (Supplemental Figure 6B). REEP1 also coimmunoprecipitated with the other human atlastin family members, atlastin-2 and atlastin-3 (Supplemental Figure 8), which are highly similar to atlastin-1 in the membrane-spanning regions but divergent in the cytoplasmic C terminus (9, 36).

Atlastin-1 binds spastin through an N-terminal domain that is only present in the larger of the 2 isoforms, M1 spastin (23, 24) (Figure 8A). Interestingly, in immunocytochemical studies, the smaller M87 spastin was mostly cytoplasmic, with some punctate labeling but little colocalization with REEP1, while M1 spastin colocalized extensively with REEP1 along bundled microtubules (Figure 8B). M1 spastin harbors a hydrophobic segment, but it has not been formally established whether or not this spastin isoform is an integral membrane protein. We performed alkaline extraction experiments and found that M87 spastin was partially extractable, but M1 spastin was not extracted at all (Figure 8C). A more clear distinction was observed in Triton X-114 detergent phase partitioning experiments, in which M87 spastin partitioned to the aqueous phase and M1 spastin to the detergent phase (Figure 8D). These data demonstrate that M1 spastin is an integral membrane protein. Since the interaction between atlastin-1 and spastin was originally identified in yeast 2-hybrid screens by 2 different groups (23, 24), we used yeast 2-hybrid tests to narrow the domain of spastin sufficient for interaction with atlastin-1 to a segment containing the hydrophobic domain. A minimal region of atlastin-1 sufficient for interaction with spastin includes the 2 very closely spaced hydrophobic segments at the atlastin-1 C terminus (Supplemental Figure 9, A–E). These paired hydrophobic segments are conserved in other atlastin family members (9), both in humans and across other species, and, in fact, an N-terminal fragment of M1 spastin that harbors its hydrophobic domain (aa 1–109) also binds to atlastin-3 (Supplemental Figure 9F). Though it was unexpected for yeast 2-hybrid studies to effectively demonstrate interactions between hydrophobic domains of different proteins, these segments may inefficiently integrate into membranes in yeast, and hydrophilic regions flanking these hydrophobic segments may also participate in these interactions (23, 24).

Since atlastin-1 interacts with the reticulons and REEP/DP1/Yop1p proteins that are characterized by novel membrane-inserted, hydrophobic hairpin structures (Figure 7 and refs. 8, 13), we inves-

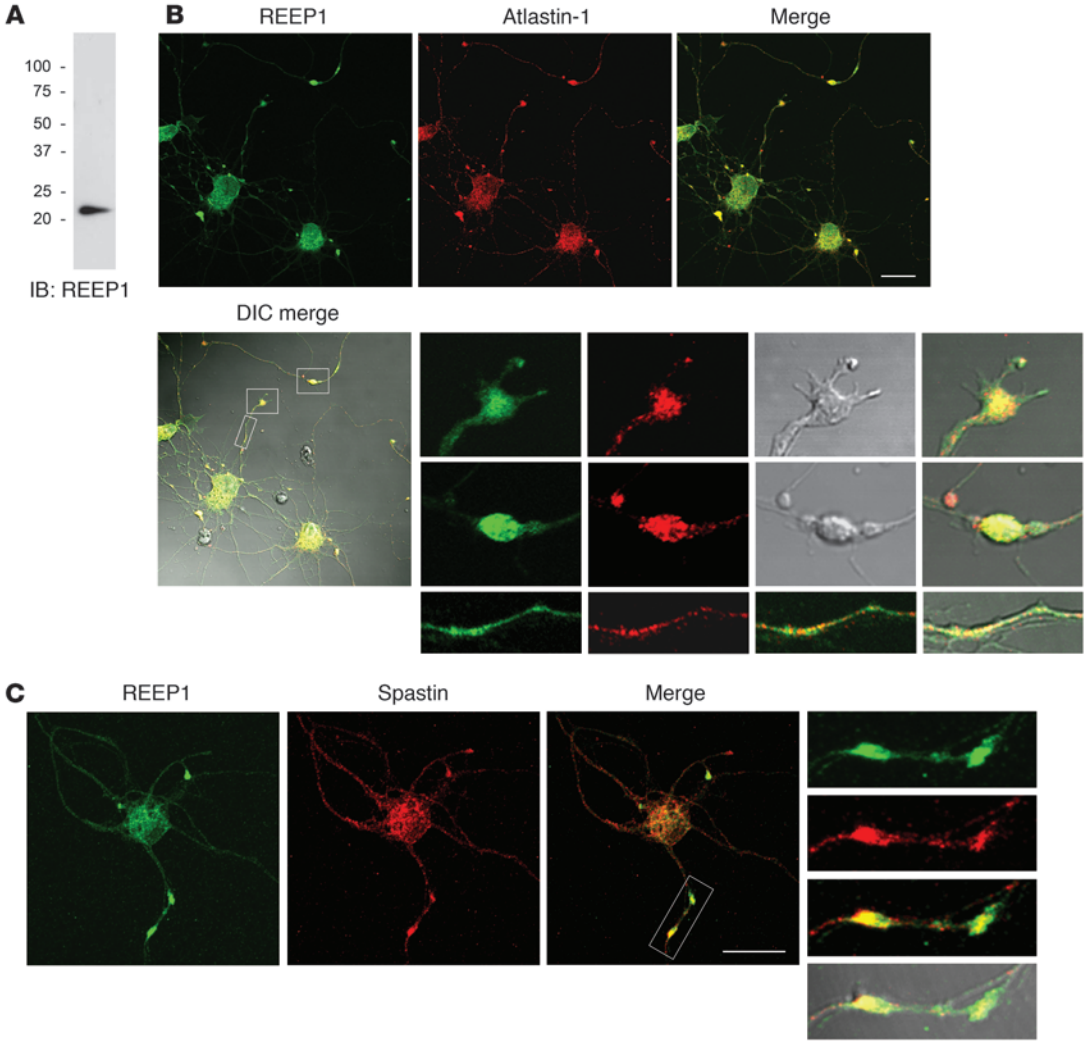

Figure 6
Endogenous REEP1 colocalizes with atlastin-1 and spastin in cerebral cortical neurons in culture. (**A**) Membranes prepared from rat cortical neurons in primary culture were immunoblotted for REEP1. (**B**) REEP1 colocalizes with atlastin-1. Neurons were costained for REEP1 (green) and atlastin-1 (red). A merged image superimposed on the DIC image is shown, and boxed areas representing areas of enrichment and colocalization in growth cones (top panels), axonal varicosities (middle panels), and the axon shaft (bottom panels) are shown in enlargements to the right (original magnification, ×4.6). (**C**) REEP1 colocalizes with spastin. Neurons were costained for REEP1 (green) and spastin (red). The boxed area shows protein enrichment and colocalization in axonal varicosities, as shown in enlargements to the right (original magnification, ×2.5). Scale bars: 20 μm.

tigated the membrane topology of M1 spastin. We found that the N terminus of M1 Myc-spastin was cytoplasmic by performing protease protection assays with intact microsomes (Figure 8E). In addition, M1 Myc-spastin G15N and Y52N mutations that create consensus *N*-linked glycosylation sites in the N-terminal region migrated identically to WT M1 spastin on immunoblots (Figure 8F), indicating that this sites are not *N*-glycosylated in cells and thus that the N terminus is likely not luminal, consistent with the protease protection data. Together, these data support the M1 spastin membrane topology diagrammed in Figure 8G, with a single intramembrane hairpin reminiscent of the double hairpins in reticulons and DP1/REEP/Yop1p proteins. In immunoprecipitation studies, REEP1 bound much more prominently to the larger M1 spastin, which includes this hydrophobic hairpin, than to the smaller M87 form (Figure 8H). In fact, the interaction of atlastin-1 with M87 spastin, evident only on longer immunoblot exposures, might conceivably be mediated indirectly through oligomerization of the M87 form with endogenous M1 spastin in the cells. Lastly, the SPG31 mutant REEP1 (aa 1–112) coimmunoprecipitated with the M1 spastin TM (aa 1–109) that contains the intramembrane hairpin, suggesting that the REEP1-M1 spastin interaction occurs through the hydrophobic domains of both proteins (Supplemental Figure 6C). Protease protection assays indicate that the membrane topology of HA-tagged spastin TM is similar to that of the full-length protein, with the N terminus oriented to the cytoplasm (Supplemental Figure 10).

A prominent difference between the REEP1–4 and REEP5–6/Yop1p protein families is the smaller size of the first hydrophobic

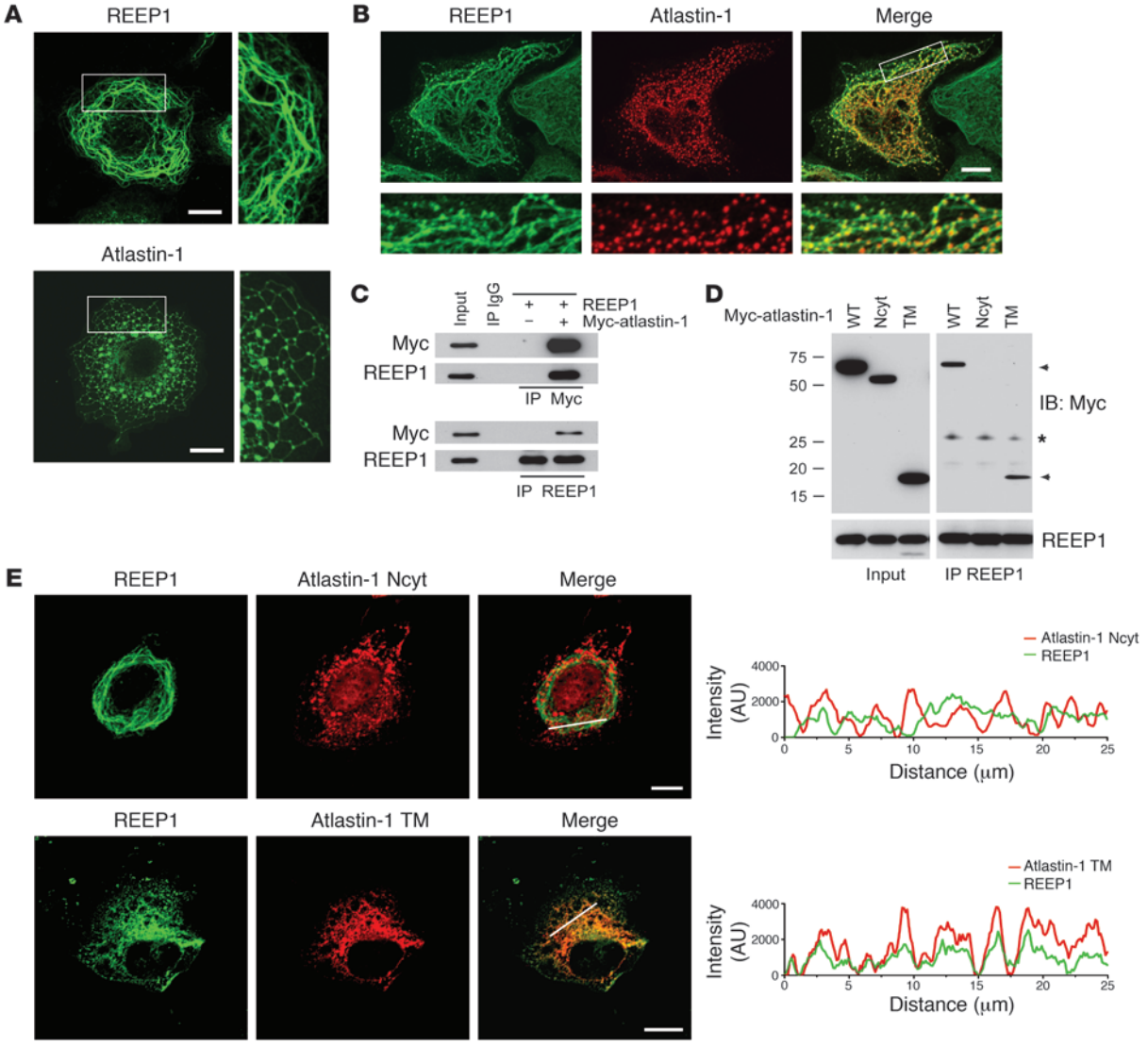

Figure 7

REEP1 interacts with atlastin-1 through intramembrane hydrophobic domains. (**A**) The ER network in COS7 cells overexpressing REEP1 and atlastin-1 alone is morphologically distinct. Boxed areas are shown in enlargements to the right (original magnification, ×2.3). (**B**) Colocalization of overexpressed REEP1 and atlastin-1 in COS7 cells. Atlastin-1 (red) immunoreactive puncta are studded along REEP1-positive (green) tubules (top panels). The boxed area is enlarged in the panels directly below (original magnification, ×3.0). (**C**) Atlastin-1 and REEP1 coimmunoprecipitate. Cells were transfected with REEP1 and Myc–atlastin-1 or REEP1 alone, immunoprecipitated with either Myc-epitope or REEP1 antibodies, and immunoblotted with Myc-epitope and REEP1 antibodies. Input and control IgG IP lanes used extracts from cells coexpressing REEP1 and Myc–atlastin-1. (**D**) Domain mapping of atlastin-1 interaction with REEP1. Myc-tagged WT atlastin-1, atlastin-1 Ncyt (aa 1–447), or atlastin-1 TM (aa 449–558) were coexpressed with REEP1 and immunoprecipitated with anti-REEP1 antibodies. Immunoprecipitates were immunoblotted for Myc-epitope or REEP1. Arrowheads identify immunoprecipitated atlastin-1 proteins, and an asterisk identifies the IgG light chain. MW standards (in kDa) are to the left. (**E**) REEP1 (green) was coexpressed with Myc–atlastin-1 Ncyt or Myc–atlastin-1 TM (red) and identified in cells using confocal immunofluorescence microscopy. REEP1 colocalizes with atlastin-1 TM but not atlastin-1 Ncyt, as shown in the merged images and as quantitated in the line scan plots. Scale bars: 20 μm.

segment in REEP1–4 relative to that in REEP5–6/Yop1p, while the second hydrophobic segment in both protein classes is of the same size, with a number of highly conserved residues (Supplemental Figures 1 and 2). Since atlastin GTPases interact with proteins in both REEP protein families, we examined whether the more divergent first hydrophobic segment of REEP1 was required for interaction with M1 spastin or atlastin. The ΔN-REEP1 protein that lacks nearly all of the first hydrophobic segment formed oligomers to a similar degree as WT REEP1 in chemical cross-linking studies (Supplemental Figure 11, A and B). Furthermore, ΔN-REEP1 coprecipitated with both atlastin-1 TM and spastin TM (Supplemental Figure 11C), indicating that the second transmembrane domain, identified previously as an intramembrane hairpin (13), likely mediates the interactions of REEP1 with atlastin-1 and spastin.

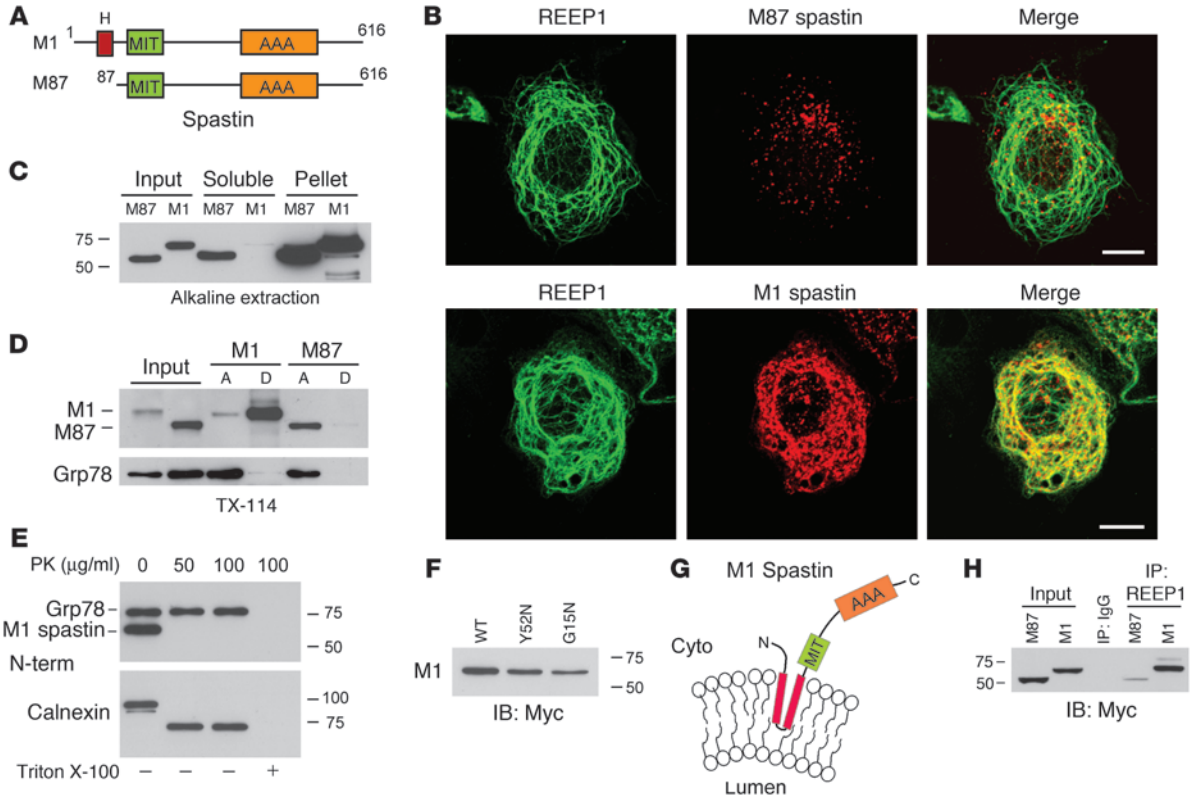

Figure 8

REEP1 interacts preferentially with the M1 isoform of spastin. (**A**) A schematic diagram showing the domain organization of spastin isoforms generated through use of 2 different translation start codons. MIT, present in microtubule-interacting and transport proteins. (**B**) REEP1 (green) was coexpressed with Myc-tagged M87 (top; red) or M1 spastin (bottom; red) and visualized using confocal microscopy. Scale bars: 10 μm. (**C**) Alkaline extraction. Myc-tagged M1 spastin but not M87 spastin is present exclusively in the pellet fraction after alkaline extraction, as revealed by immunoblotting for Myc-epitope. MW standards (in kDa) are indicated throughout. (**D**) Detergent phase partitioning. Membranes from M1 and M87 spastin-expressing cells were partitioned with Triton X-114 (TX-114). Input membranes as well as aqueous (A) and detergent (D) phases were immunoblotted. Partitioning of the soluble protein Grp78 is shown for comparison. (**E**) Protease protection. Proteinase K was added to intact microsomes from Myc-tagged M1 spastin-expressing cells, with or without Triton X-100, and aliquots were immunoblotted for M1 spastin (Myc-epitope), Grp78, and calnexin. (**F**) M1 spastins Y52N and G15N create consensus *N*-linked glycosylation sites but are not glycosylated. WT and the indicated mutant M1 spastin proteins were expressed in COS7 cells and immunoblotted for Myc. (**G**) Model for REEP1 membrane topology. (**H**) M1 spastin and REEP1 coimmunoprecipitate. Cells were cotransfected with REEP1 and either Myc-tagged M1 or M87 spastin, then immunoprecipitated with anti-REEP1 antibodies and immunoblotted with anti–Myc-epitope antibodies. The control IgG IP lane used extracts from cells coexpressing REEP1 and M1 spastin.

Unexpectedly, ΔN-REEP1, when coexpressed with spastin TM or atlastin-1 TM, did not result in the expected pattern of altered ER tubules aligned along bundled microtubules, even though it localized to the tubular ER, indicating that the first hydrophobic domain is important for maintaining REEP1 structure or mediating other interactions that are important for REEP1 interaction with microtubules in cells (Supplemental Figure 11D). Similarly, tagging full-length REEP1 at the N terminus with Myc epitope or HA epitope resulted in the same ER phenotype as seen upon expression of ΔN-REEP1 (data not shown), consistent with a structural disruption of the intramembrane first hydrophobic segment by the hydrophilic epitope tag.

Discussion

Though over 40 genetic loci for the HSPs have been identified, most cases of pure HSP result from autosomal dominant mutations in 1 of just 3 genes: *SPG3A*, *SPG4*, and *SPG31*. Our recent studies have emphasized the formation of interconnections among ER tubules mediated by the atlastin GTPases through interactions with proteins of the DP1/Yop1p and reticulon superfamilies (8, 9). Since the atlastin-1 protein interacts with DP1/REEP5, and REEP1 is in the same protein superfamily based on sequence similarity, we hypothesized that REEP1 might be involved in a common cellular pathway with atlastin-1 (8). In fact, both SPG3A and SPG31 are notable for being early-onset HSPs, in contrast to most other known forms (33, 37). Furthermore, the SPG4 protein spastin interacts with atlastin-1 as well as with members of the reticulon family of ER-shaping proteins (38), indicating that the 3 most common HSP proteins — atlastin-1, REEP1, and spastin — might have interrelated roles in forming the ER network.

In this study, we demonstrate that atlastin-1, the M1 isoform of spastin, and REEP1 interact with one another through hydrophobic hairpin domains within the tubular ER to coordinate ER shaping and microtubule interactions (Figure 9). Interestingly, each of these

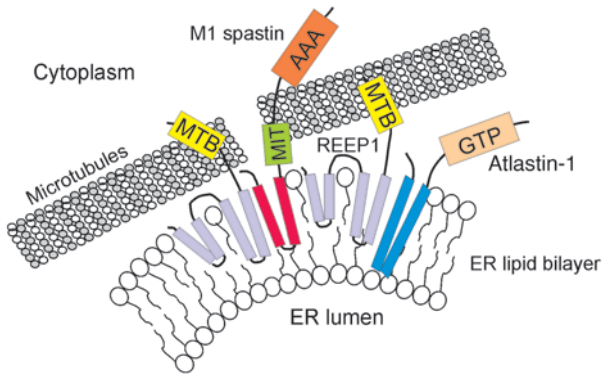

Figure 9

Model for interactions among the HSP proteins in the tubular ER. In this schematic diagram, atlastin-1 and M1 spastin interact directly with the ER-shaping proteins, including REEP1, as well as with one another (not shown). These interactions very likely occur through the hydrophobic hairpins of each of these proteins inserted into the membrane, though the first hydrophobic domain may exist in the ER membrane instead as a more traditional transmembrane segment (see Figure 1J). It is unclear whether the larger atlastin-1 hydrophobic segments completely span the membrane. REEP1 makes direct contact with the microtubule cytoskeleton through its C-terminal cytoplasmic domain. The M1 isoform of the spastin ATPase also binds to microtubules, through the MIT domain or a region adjacent to it, and is involved in microtubule severing, coupling changes in ER morphology with microtubule dynamics. GTP, GTP-binding domain; MTB, microtubule-binding domain.

proteins is enriched in the central nervous system, and in particular within the cell bodies and axons of corticospinal neurons whose axons are impaired in the HSPs (Figure 6 and refs. 17, 20, 22). Atlastin-1 and REEP1 are likely members of larger protein families, atlastin-1–3 and REEP1–4, respectively, with similar functions. The fact that atlastin-1, REEP1, and M1 spastin are particularly enriched in the central nervous system may contribute to the selectivity of the neurological involvement in this class of disorders.

Our study emphasizes the interactions of these HSP proteins within cells as well as how they contribute to the formation of the tubular ER network and its interactions with the microtubule cytoskeleton. The localization of REEP1 has been controversial, with recent reports indicating that it is mitochondrial instead of within the ER (31). We have established that REEP1 is a member of the DP1/Yop1p family of ER-shaping proteins that interacts with both atlastin-1 and M1 spastin, giving rise to a protein complex with pathogenic significance for a majority of HSP cases. Unexpectedly, REEP1 also mediates interaction of ER tubules with the microtubule cytoskeleton through its C-terminal cytoplasmic domain, and in fact defines a novel family within the larger DP1/Yop1p superfamily. In this regard, the ER phenotype upon REEP1 overexpression, characterized by ER tubules closely aligned with thickened, bundled microtubules, is similar to that observed for the *SPG4* missense mutant spastin p.K388R that lacks ATPase activity and microtubule-severing activity but retains the ability to bind microtubules (25, 26). Furthermore, both REEP1 and spastin interact with atlastin-1 as well as ER-shaping proteins, such as the reticulons (present study and refs. 23, 24, 38).

Since interactions among DP1/Yop1p and reticulon family members occur through proposed paired intramembrane hairpin domains, and this region also interacts with the tightly paired hydrophobic domains of the atlastins (8, 13), we examined the membrane-spanning topology of M1 spastin, which binds atlastins as well as REEP1. We found that the hydrophobic segment of M1 spastin similarly sits in the membrane as a partially membrane-spanning hairpin. Since the paired hydrophobic domains of each of these HSP proteins are necessary and sufficient for their localization to the tubular ER (8), this motif may function as a dual membrane-sorting signal and protein interaction motif.

Though the microtubule cytoskeleton is not required for ER network formation, tubules are often pulled out by their associations with the tips of microtubules or actin filaments as they polymerize, via motor proteins along microtubule tracks, or else through interactions with moving microtubules (39, 40). Our finding that REEP1, like spastin, interacts with the microtubule cytoskeleton suggests an important role for the microtubule cytoskeleton in the distribution of the ER network, which is particularly relevant for the long axonal processes of highly polarized corticospinal motor neurons that can extend up to 1 meter in length in humans (3). Interestingly, though REEP1 and the closely related protein REEP2 interact with microtubules and redistribute ER tubules along the microtubule cytoskeleton, DP1/REEP5 and REEP6 do not (present study and refs. 15, 30). It will be important to determine in future studies whether microtubule interactions are a general feature of all members of REEP1–4 that distinguishes them from REEP5–6. Indeed, such an adaptation may reflect the increased importance of ER-microtubule interactions in forming and distributing the ER network in higher species, particularly within highly polarized cells, such as the corticospinal neurons that are selectively affected in the HSPs. Along these lines, the budding yeast *S. cerevisiae* has only 1 DP1/Yop1p superfamily member, Yop1p, which is structurally and functionally related to REEP5–6 proteins. Since *S. cerevisiae* generates ER tubules along actin filaments, there may be no need for a REEP1–4 ortholog.

The SPG31 mutant REEP1 that we investigated here exemplifies a probable functional uncoupling with pathogenic significance, since it possesses the hydrophobic hairpin domain important for oligomerization, interactions with atlastins and M1 spastin, and shaping ER tubules (8, 13, 14, 41) but lacks the ability to interact with microtubules. In fact, we have shown that the C-terminal tail of REEP1 is both necessary and sufficient for interaction with microtubules. As a result, though an ER network is present in the truncated SPG31 mutant REEP1, there are far fewer interconnections and a more sheet-like appearance in many areas. Interestingly, atlastin-1 does not interact with CLIMP-63 (8), another ER membrane protein that binds microtubules but is present endogenously mainly in rough ER sheets and whose overexpression results in the proliferation of ER sheets (11, 42, 43), in contrast to REEP1. Thus, REEP1 and CLIMP-63 may have analogous functions in mediating microtubule-ER interactions in different ER subdomains.

SPG4 is the most common form of HSP and is caused by loss-of-function mutations in the gene encoding spastin, a microtubule-severing AAA ATPase that interacts with microtubules, atlastin-1, and REEP1 and which is important for axon growth and branching (20–23). Though spastin has microtubule-severing activities that are important for cytokinesis, these involve the smaller M87 isoform (25, 44), while interactions with atlastin-1 and REEP1 involve the larger M1 isoform. M1 spastin is particularly enriched in spinal cord (20, 22), the location of the corticospinal axons affected in the HSPs, and overexpression of a dysfunctional M1 polypeptide (but not a M87 polypeptide) interferes with normal

axonal growth and transport, highlighting the likely role of the M1 spastin isoform in disease pathogenesis (20).

The relationship between atlastin GTPases and microtubule-severing AAA ATPases in the establishment and maintenance of long cellular processes appears to be evolutionarily conserved across a wide range of organisms. For instance, some epidermal cells in the roots of higher plants have long, tubular outgrowths, known as root hairs that are reminiscent of neurites in animal cells. As for neuronal axons (17), root hair tip growth in the plant *Arabidopsis* is also dependent on microtubules (45) and similarly inhibited by loss-of-function mutants of the atlastin-1 ortholog RHD3 (46). Furthermore, *rhd3* loss-of-function mutations suppress an *Arabidopsis* phenotype characterized by root waving, skewing, and epidermal cell file rotation when plants are grown on a tilted agar surface. Importantly, mutations in the *erh3* gene encoding a microtubule-severing, AAA ATPase also suppress this phenotype (47). Lastly, in *Drosophila* muscle cells, atlastin (*atl*; *spg3a*) functions with spastin to disassemble microtubules, and the microtubule-destabilizing drug vinblastine alleviates synaptic and muscular defects in *atl* mutant flies (48) as well as neuromuscular junction and locomotor abnormalities in *spas* (*Dspastin*) mutant flies (49). Together, these studies support a fundamental link between microtubule-severing ATPases and atlastins in the regulation of ER morphology and the formation and maintenance of long cellular processes. Coupled with our data showing a functional relationship between the atlastins and spastin with ER-shaping proteins, including REEP1 (present study and ref. 8), the interactions of the HSP proteins atlastin-1, REEP1, and spastin with one another strongly supports a convergent mechanism of disease.

We considered the possibility that morphological changes in neuronal organelles other than the tubular ER may be involved in HSP pathogenesis, since these 3 HSP proteins might also be present to varying degrees in such structures as tubular domains of ERGIC (17, 50), or the highly curved edges of ER sheets (16), or even the *cis*-Golgi apparatus. In fact, the Golgi apparatus is fragmented when atlastin is depleted in some *Drosophila* and mammalian cells, though secretory function is largely preserved, as well as upon REEP1 overexpression (present study and refs. 9, 48, 51). In these cases, the microtubule network is also disrupted. Since Golgi fragmentation into mini-stacks is seen upon microtubule disruption, using the microtubule-destabilizing drug nocodazole (52), these atlastin and REEP1-dependent changes in Golgi morphology likely represent secondary effects. Importantly, the vast majority of cellular atlastin, M1 spastin, and REEP proteins are found within the tubular ER.

Thus, we postulate that the most common HSPs — involving SPG3A, SPG4, and SPG31 proteins — are fundamentally diseases of ER network disruption, particularly as it relates to interactions with the microtubule cytoskeleton. We suspect that these HSP proteins function cooperatively to regulate polarized membrane and protein trafficking along microtubules to distant sites within cells (50, 53) and that disruption of these processes particularly affects the long axons of the corticospinal neurons, which are among the longest axons in the body, in a length-dependent manner. Thus, HSP pathogenesis may be related to defects in the spatial distribution of proteins or membranes that result from fundamental defects in ER organization within the cell. Further studies investigating the functional role of these HSP proteins and their interactions in axon development and maintenance in neurons will advance our understanding of HSP pathogenesis.

Methods

DNA constructs. The human REEP1 coding sequence (GenBank NM_022912) was cloned into the *Eco*RI site of the eukaryotic expression vector pRK5 (Genentech). ΔN-REEP was generated by deleting the nucleotides generating residues 1–20 and replacing Phe21 with an initiator Met before cloning into pRK5. Expression constructs for human atlastins and both GFP- and RFP-Sec61β have been described previously (8, 9, 15, 36). Human spastin M1 and M87 isoforms (GenBank NM_014946) were cloned into the *Eco*RI site of pGW1-Myc, which incorporates an N-terminal Myc-epitope tag. The pDsRed2-Mito plasmid was purchased from Clontech. Mutant REEP1 (aa 1–112) was generated by PCR amplification and cloned into the *Hind*III and *Bgl*II sites of a modified pGW1 eukaryotic expression vector with an in-frame, C-terminal HA-epitope tag (36). REEP1, REEP2 (GenBank NM_016606), REEP5 (GenBank NM_005669), and REEP6 (GenBank NM_138393) were also cloned into the *Hind*III and *Bgl*II sites of the same vector to generate a recombinant protein with an in-frame, C-terminal HA-epitope tag. REEP1 (aa 113–201) was generated by PCR amplification and cloned into the *Eco*RI site of pGEX-6P-1.

Antibodies. An atlastin-1 mouse monoclonal antibody (clone 3194) was generated commercially (ProMab Biotechnologies) against a synthetic peptide corresponding to residues 1–18 of human atlastin-1 (36) and affinity purified. Polyclonal antibodies against human REEP1 (GenBank NP_075063; residues 174–191) were raised in rabbits and affinity purified (Veritas). The following antibodies were obtained commercially: mouse monoclonal anti-TRAPα (IgG_1; Abcam), rabbit polyclonal anti-IP_3R (Abcam), mouse monoclonal anti–β-tubulin (IgG_1, clone D66; Sigma-Aldrich), mouse monoclonal anti-spastin (IgG_{2a}, clone Sp 6C6; Sigma-Aldrich), mouse monoclonal p115 (IgG_1, clone 15; BD Biosciences — Pharmingen), mouse monoclonal anti-cytochrome *c* (IgG_1, clone 6H2.B4; BD Biosciences), rabbit polyclonal anti-HA probe (Y-11; Santa Cruz Biotechnology Inc.), mouse monoclonal anti–Myc-epitope (IgG_1, clone 9E10; Santa Cruz Biotechnology Inc.), mouse monoclonal anti-calnexin (IgG_1, clone 37; BD Biosciences — Transduction Laboratories), and mouse monoclonal anti-BiP/Grp78 (IgG_{2a}, clone 40; BD Biosciences — Transduction Laboratories).

Tissue culture, immunoprecipitation, gel electrophoresis, and immunoblotting. Homogenates were prepared from adult male Sprague Dawley rats (150–175 g; Charles River Laboratories) as described previously (36). COS7, HEK293, and HeLa cells were maintained as described previously (9, 36, 54), and DNA vector transfections were performed with GenJet Plus (SignaGen Laboratories) 24 hours after transfection. For RNA interference studies, HEK293 cells were transfected REEP1-specific siRNA (HSS127948; Invitrogen) or control siRNA as described previously (9). Immunoprecipitations were conducted essentially as described (36) but with the use of protein A/G PLUS-agarose beads (Santa Cruz Biotechnology Inc.). Procedures for preparation of cell extracts, SDS-PAGE, and immunoblotting have been described previously (36). Two-dimensional gel electrophoresis was performed as described by Lee et al. (55).

Biochemical studies. Membrane association, Triton X-114 phase partitioning, and protease protection assays were performed as described previously (9, 36). Chemical cross-linking with 1 mM DSP was performed in PBS, essentially as described by Zhu et al. (36), except that the cross-linker was incubated for 2 hours at 4°C. Where indicated, 1 mM DTT was added to cleave the cross-links.

In vitro ER network formation. Anti-REEP antibodies were prepared commercially against acetyl-CADSDSMDERWSDSEIAETRT-amide (GenBank NP_001086898; residues 191–210) and acetyl-CGLRRSQSMRSVKVIKGRKEIRY-amide (*Xenopus*, GenBank NP_001088957; residues 216–237) (Supplemental Figure 2) and affinity purified. The N-terminal Cys residue was added to facilitate coupling to the keyhole limpet hemocyanin (21st Century Biochemicals). ER network formation was performed

in vitro from *Xenopus* egg membranes as described previously (8). For the network formation assay, affinity-purified anti-REEP antibodies raised in rabbits against 2 regions highly conserved among known *Xenopus* REEPs were used at 1.1 μM. Equimolar rabbit IgG (Sigma-Aldrich), as well as antibodies against the resident ER membrane proteins anti-IP_3R and anti-TRAPα, were used as controls.

Immunofluorescence staining and confocal microscopy. Immunofluorescence staining of paraformaldehyde-fixed COS7, HEK293, and HeLa cells was performed as described previously (9, 44, 54). Cells were imaged using a Zeiss LSM510 confocal microscope with a 63× 1.4 NA Plan-APOCHROMAT lens. Acquisition was performed with LSM510 version 3.2 SP2 software (Carl Zeiss Microimaging), and data were processed using Adobe Illustrator CS2 and Photoshop 7.0 software. All animal care and experimental procedures were approved by the NINDS/National Institute on Deafness and other Communication Disorders Animal Care and Use Committee (NIH). Rat cerebral cortical neurons were prepared and maintained in primary culture and then fixed and immunostained at 6 days in vitro as described previously (17).

Microtubule cosedimentation assays. To examine the REEP1-microtubule interaction in vivo, HEK293 cells were collected 24 hours after transfection and lysed in 80 mM PIPES (pH 7.0), 1 mM $MgCl_2$, 0.5 mM EGTA, and 1.0% Triton X-100 plus protease inhibitors. After multiple passages through a 30-gauge needle, samples were incubated on ice for 30 minutes and then centrifuged (610 *g*; 10 minutes at 4°C). The supernatant was collected and incubated with 40 μM paclitaxel and 1 mM GTP in DMSO or else equimolar DMSO alone for 30 minutes at 37°C. Samples were layered over a 50% glycerol cushion containing 80 mM PIPES (pH 7.0), 1 mM $MgCl_2$, and 0.5 mM EGTA and then centrifuged at 100,000 *g* at 4°C for 40 minutes. Precipitate and supernatant fractions were collected for immunoblot analysis. To examine the REEP1-microtubule interaction in vitro, GST and GST-REEP1 were produced in bacteria and affinity purified using the B-PER GST fusion protein spin purification kit (Pierce) and then assessed using the microtubule-binding spin down assay kit (Cytoskeleton Inc.). Pellet and supernatant fractions were analyzed by immunoblotting.

Yeast 2-hybrid assays. Yeast 2-hybrid assays using the AH109 yeast strain were performed as described previously (9). Bait constructs for spastin were generated by PCR amplification and cloned into the pGBKT7 vector (BD Biosciences Clontech), while atlastin-1 and atlastin-3 prey constructs were generated by PCR amplification and cloned into the pGAD10 prey vector (BD Biosciences Clontech).

Protein content determination. Protein concentrations were assessed using the bicinchoninic acid assay kit (Pierce), with BSA as the standard.

Statistics. Statistical analyses were performed using Student's *t* test, assuming unequal variance. *P* values of less than 0.05 were considered significant.

Acknowledgments

We thank J. Nagle and D. Kauffman (NINDS DNA Sequencing Facility) for DNA sequencing, J. Stadler for technical assistance, and T.A. Rapoport and Y. Shibata for valuable discussions and critical review of the manuscript. R.L. Parker was supported by the Howard Hughes Medical Institute-NIH Research Scholars Program. This research was supported by the Intramural Research Program of the NINDS, NIH.

Received for publication August 27, 2009, and accepted in revised form January 6, 2010.

Address correspondence to: Craig Blackstone, Cellular Neurology Unit, Neurogenetics Branch, National Institute of Neurological Disorders and Stroke, NIH, Building 35, Room 2C-913, 9000 Rockville Pike, Bethesda, MD 20892-3738. Phone: 301.451.9680; Fax: 301.480.4888; E-mail: blackstc@ninds.nih.gov.

Rell L. Parker's present address is: Division of Biology, California Institute of Technology, Pasadena, California, USA.

1. Reid E. Science in motion: common molecular pathological themes emerge in the hereditary spastic paraplegias. *J Med Genet*. 2003;40(2):81–86.
2. Fink JK. Hereditary spastic paraplegia. *Curr Neurol Neurosci Rep*. 2006;6(1):65–76.
3. Soderblom C, Blackstone C. Traffic accidents: molecular genetic insights into the pathogenesis of the hereditary spastic paraplegias. *Pharmacol Ther*. 2006;109(1–2):42–56.
4. Züchner S. The genetics of hereditary spastic paraplegia and implications for drug therapy. *Expert Opin Pharmacother*. 2007;8(10):1433–1439.
5. Salinas S, Proukakis C, Crosby A, Warner TT. Hereditary spastic paraplegia: clinical features and pathogenetic mechanisms. *Lancet Neurol*. 2008; 7(12):1127–1138.
6. Harding AE. Classification of the hereditary ataxias and paraplegias. *Lancet*. 1983;1(8334):1151–1155.
7. Dürr A. Genetic testing for the spastic paraplegias: drowning by numbers. *Neurology*. 2008; 71(4):236–238.
8. Hu J, et al. A class of dynamin-like GTPases involved in the generation of the tubular ER network. *Cell*. 2009; 138(3):549–561.
9. Rismanchi N, Soderblom C, Stadler J, Zhu P-P, Blackstone C. Atlastin GTPases are required for Golgi apparatus and ER morphogenesis. *Hum Mol Genet*. 2008;17(11):1591–1604.
10. Orso G, et al. Homotypic fusion of ER membranes requires the dynamin-like GTPase atlastin. *Nature*. 2009;460(7258):978–983.
11. Shibata Y, Voeltz GK, Rapoport TA. Rough sheets and smooth tubules. *Cell*. 2006;126(3):435–439.
12. English AR, Zurek N, Voeltz GK. Peripheral ER structure and function. *Curr Opin Cell Biol*. 2009; 21(4):596–602.
13. Voeltz G, Prinz WA, Shibata Y, Rist JM, Rapoport TA. A class of membrane proteins shaping the tubular endoplasmic reticulum. *Cell*. 2006;124(3):573–586.
14. Hu J, et al. Membrane proteins of the endoplasmic reticulum induce high-curvature tubules. *Science*. 2008;319(5867):1247–1250.
15. Shibata Y, et al. The reticulon and DP1/Yop1p proteins form immobile oligomers in the tubular endoplasmic reticulum. *J Biol Chem*. 2008; 283(27):18892–18904.
16. Shibata Y, Hu J, Kozlov MM, Rapoport TA. Mechanisms shaping the membranes of cellular organelles. *Annu Rev Cell Dev Biol*. 2009;25:329–354.
17. Zhu P-P, Soderblom C, Tao-Cheng J-H, Stadler J, Blackstone C. SPG3A protein atlastin-1 is enriched in growth cones and promotes axon elongation during neuronal development. *Hum Mol Genet*. 2006; 15(8):1343–1353.
18. Errico A, Ballabio A, Rugarli EI. Spastin, the protein mutated in autosomal dominant hereditary spastic paraplegia, is involved in microtubule dynamics. *Hum Mol Genet*. 2002;11(2):153–163.
19. Roll-Mecak A, Vale RD. The Drosophila homologue of the hereditary spastic paraplegia protein, spastin, severs and disassembles microtubules. *Curr Biol*. 2005;15(7):650–655.
20. Solowska JM, et al. Quantitative and functional analyses of spastin in the nervous system: implications for hereditary spastic paraplegia. *J Neurosci*. 2008;28(9):2147–2157.
21. Riano E, et al. Pleiotropic effects of spastin on neurite growth depending on expression levels. *J Neurochem*. 2009;108(5):1277–1288.
22. Claudiani P, Riano E, Errico A, Andolfi G, Rugarli EI. Spastin subcellular localization is regulated through usage of different translation start sites and active export from the nucleus. *Exp Cell Res*. 2005; 309(2):358–369.
23. Evans K, Keller C, Pavur K, Glasgow K, Conn B, Lauring B. Interaction of two hereditary spastic paraplegia gene products, spastin and atlastin, suggests a common pathway for axonal maintenance. *Proc Natl Acad Sci U S A*. 2006;103(28):10666–10671.
24. Sanderson CM, et al. Spastin and atlastin, two proteins mutated in autosomal-dominant hereditary spastic paraplegia, are binding partners. *Hum Mol Genet*. 2006;15(2):307–318.
25. Connell JW, Lindon C, Luzio JP, Reid E. Spastin couples microtubule severing to membrane traffic in completion of cytokinesis and secretion. *Traffic*. 2009; 10(1):42–56.
26. Yabe I, Sasaki H, Tashiro K, Matsuura T, Takegami T, Satoh T. Spastin gene mutation in Japanese with hereditary spastic paraplegia. *J Med Genet*. 2002; 39(8):e46.
27. Barlowe C. Atlastin GTPases shape up ER networks. *Dev Cell*. 2009;17(2):157–158.
28. Farhan H, Hauri H-P. Networking at the ER with atlastin. *Curr Biol*. 2009;19(19):R906–R908.
29. Saito H, Kubota M, Roberts RW, Chi Q, Matsunami H. RTP family members induce functional expression of mammalian odorant receptors. *Cell*. 2004; 119(5):679–691.
30. Behrens M, et al. Members of RTP and REEP gene families influence functional bitter taste receptor expression. *J Biol Chem*. 2006;281(29):20650–20659.
31. Züchner S, et al. Mutations in the novel mitochondrial protein REEP1 cause hereditary spastic paraplegia type 31. *Am J Hum Genet*. 2006;79(2):365–369.

32. Dreier L, Rapoport TA. In vitro formation of the endoplasmic reticulum occurs independently of microtubules by a controlled fusion reaction. *J Cell Biol*. 2000;148(5):883–898.
33. Beetz C, et al. REEP1 mutation spectrum and genotype/phenotype correlation in hereditary spastic paraplegia type 31. *Brain*. 2008;131(Pt 4):1078–1086.
34. Schlang KJ, Arning L, Epplen JT, Stemmler S. Autosomal dominant hereditary spastic paraplegia: novel mutations in the REEP1 gene (SPG31). *BMC Med Genet*. 2008;9:71.
35. Hewamadduma C, et al. New pedigrees and novel mutation expand the phenotype of *REEP1*-associated hereditary spastic paraplegia (HSP). *Neurogenetics*. 2009;10(2):105–110.
36. Zhu P-P, et al. Cellular localization, oligomerization, and membrane association of the hereditary spastic paraplegia 3A (SPG3A) protein atlastin. *J Biol Chem*. 2003;278(49):49063–49071.
37. Namekawa M, et al. SPG3A is the most frequent cause of hereditary spastic paraplegia with onset before age 10 years. *Neurology*. 2006;66(1):112–114.
38. Mannan AU, et al. Spastin, the most commonly mutated protein in hereditary spastic paraplegia interacts with reticulon 1 an endoplasmic reticulum protein. *Neurogenetics*. 2006;7(2):93–103.
39. Prinz WA, Grzyb L, Veenhuis M, Kahan JA, Silver PA, Rapoport TA. Mutants affecting the structure of the cortical endoplasmic reticulum in Saccharomyces cerevisiae. *J Cell Biol*. 2000;150(3):461–474.
40. Waterman-Storer CM, Salmon ED. Endoplasmic reticulum membrane tubules are distributed by microtubules in living cells using three distinct mechanisms. *Curr Biol*. 1998;8(14):798–806.
41. Tolley N, et al. Overexpression of a plant reticulon remodels the lumen of the cortical endoplasmic reticulum but does not perturb protein transport. *Traffic*. 2008;9(1):94–102.
42. Klopfenstein DR, Kappeler F, Hauri H-P. A novel direct interaction of endoplasmic reticulum with microtubules. *EMBO J*. 1998;17(21):6168–6177.
43. Klopfenstein DR, Klumperman J, Lustig A, Kammerer RA, Oorschot V, Hauri H-P. Subdomain-specific localization of CLIMP-63 (p63) in the endoplasmic reticulum is mediated by its luminal α-helical segment. *J Cell Biol*. 2001;153(6):1287–1300.
44. Yang D, Rismanchi N, Renvoisé B, Lippincott-Schwartz J, Blackstone C, Hurley JH. Structural basis for midbody targeting of spastin by the ESCRT-III protein CHMP1B. *Nat Struct Mol Biol*. 2008; 15(12):1278–1286.
45. Sieberer BJ, Ketelaar T, Esseling JJ, Emons AMC. Microtubules guide root hair tip growth. *New Phytologist*. 2005;167(3):711–719.
46. Wang H, Lee MM, Schiefelbein JW. Regulation of the cell expansion gene RHD3 during Arabidopsis development. *Plant Physiol*. 2002;129(2):638–649.
47. Yuen CYL, Sedbrook JC, Perrin RM, Carroll KL, Masson PH. Loss-of-function mutations of ROOT HAIR DEFECTIVE3 suppress root waving, skewing, and epidermal cell file rotation in Arabidopsis. *Plant Physiol*. 2005;138(2):701–714.
48. Lee M, et al. Drosophila atlastin regulates the stability of muscle microtubules and is required for synapse development. *Dev Biol*. 2009;330(2):250–262.
49. Orso G, Martinuzzi A, Rossetto MG, Sartori E, Feany M, Daga A. Disease-related phenotypes in a Drosophila model of hereditary spastic paraplegia are ameliorated by treatment with vinblastine. *J Clin Invest*. 2005;115(11):3026–3034.
50. Sannerud R, et al. Rab1 defines a novel pathway connecting the pre-Golgi intermediate compartment with the cell periphery. *Mol Biol Cell*. 2006;17(4):1514–1526.
51. Namekawa M, et al. Mutations in the SPG3A gene encoding the GTPase atlastin interfere with vesicle trafficking in the ER/Golgi interface and Golgi morphogenesis. *Mol Cell Neurosci*. 2007;35(1):1–13.
52. Cole NB, Sciaky N, Marotta A, Song J, Lippincott-Schwartz J. Golgi dispersal during microtubule disruption: regeneration of Golgi stacks at peripheral endoplasmic reticulum exit sites. *Mol Biol Cell*. 1996; 7(4):631–650.
53. Marie M, Sannerud R, Avsnes Dale H, Saraste J. Take the 'A' train: on fast tracks to the cell surface. *Cell Mol Life Sci*. 2008;65(18):2859–2874.
54. Rismanchi N, Puertollano R, Blackstone C. STAM adaptor proteins interact with COPII complexes and function in ER-to-Golgi trafficking. *Traffic*. 2009; 10(2):201–217.
55. Lee YM, et al. Oxidative modification of peroxiredoxin is associated with drug-induced apoptotic signaling in experimental models of Parkinson disease. *J Biol Chem*. 2008;283(15):9986–9998.